

Photocurrent Enhancement for Polymer Langmuir–Blodgett Monolayers Containing Ruthenium Complex by Surface Plasmon Resonance

Nobuko Fukuda, Masaya Mitsuishi, Atsushi Aoki, and Tokuji Miyashita*

*Institute of Multidisciplinary Research for Advanced Materials, Tohoku University,
Katahira 2-1-1, Aoba-ku, Sendai 980-8577 Japan*

Received: December 18, 2001; In Final Form: May 1, 2002

This paper describes effective photocurrent generation based on a polymer Langmuir–Blodgett (LB) monolayer containing ruthenium complex on a silver electrode excited by surface plasmon resonance (SPR). It was found that photocurrent generation is greatly enhanced at an incident angle where the electromagnetic field was most enhanced by SPR. At this angle, the photocurrent is enhanced by a factor of 23.6 compared with that at the critical angle for total internal reflection. The incident monochromatic photon-to-current conversion efficiency was $9.53 \times 10^{-3}\%$, higher than that of the corresponding polymer LB monolayer film on a transparent indium tin oxide electrode with conventional direct transmitted light ($2.87 \times 10^{-3}\%$). Furthermore, it was demonstrated that precoating with poly(*N*-dodecylacrylamide) homopolymer ensures adequate separation of the $\text{Ru}(\text{bpy})_3^{2+}$ and silver surface, thereby suppressing the quenching of photoexcited $\text{Ru}(\text{bpy})_3^{2+}$ by the silver. Controlling the distance between the $\text{Ru}(\text{bpy})_3^{2+}$ layer and the silver using the Langmuir–Blodgett technique leads to effective photoexcitation of $\text{Ru}(\text{bpy})_3^{2+}$ by SPR and suppression of quenching by the silver surface, resulting in efficient photocurrent generation.

Introduction

Surface plasmon resonance (SPR) has been widely employed as a powerful analytical tool for optical devices for the purpose of characterization of ultrathin films^{1,2} and direct monitoring for interfacial binding such as adsorption/desorption processes.^{3–7} These applications are based on the high sensitivity of the resonance angle at which free electrons in the metal layer are coupled with the incident light, allowing minute changes in the optical parameters of dielectrics deposited on metal surfaces to be detected with high accuracy. However, conventional SPR devices have some limitations, particularly with respect to the detection of adsorption events for small molecules. Recently, fluorescent spectroscopy has been combined with SPR to utilize the enhancement of the electromagnetic field at the metal surface, enabling small molecules to be detected easily via fluorescence when the molecules exhibit luminescence.^{8,9} This implies that chromophores are efficiently excited by surface plasmons. In fact, the use of evanescent optical fields has become an important issue for optical device applications.

The tris(2,2'-bipyridine)ruthenium complex ($\text{Ru}(\text{bpy})_3^{2+}$) is a well-known redox-active photosensitizer with a large molar absorption coefficient in the visible light region and has often been used in photoelectric conversion systems such as a photoelectrochemical cell.^{10–15} The driving force of photoelectric conversion is electron transfer between photoexcited $\text{Ru}(\text{bpy})_3^{2+}$ and various electron donors and acceptors, resulting in the generation of anodic and cathodic photocurrent. We have previously reported the generation of anodic photocurrent by visible light irradiation on nanoassembled amphiphilic polymer Langmuir–Blodgett (LB) films containing $\text{Ru}(\text{bpy})_3^{2+}$ derivatives on transparent electrodes in the presence of thiosalicylic acid^{16–18} or triethanolamine (TEOA)¹⁹ as sacrificial electron donors. The anodic photocurrent depends on the concentration of donors, light power, and the film structures such as hetero-

deposition of LB films of $\text{Ru}(\text{bpy})_3^{2+}$ copolymer and ferrocene copolymer as an electron donor.¹⁹ These findings are based on the fact that the functional groups are assembled regularly on a molecular scale by the LB technique.

To design a more effective photoelectric conversion, it is necessary to not only select suitable redox couples but also to improve the overall photocurrent generation system. Recently, we reported that the coupling of the LB film of the $\text{Ru}(\text{bpy})_3^{2+}$ copolymer with the surface plasmon electric field results in effective photoelectric conversion, where the metal layer provides strong excitation of the chromophores at the interface of metal/dielectrics and acts also as an electrode.²⁰ When surface plasmons are resonated, the electromagnetic field at the metal surface is enhanced remarkably, as described by Fresnel's theory.^{1,8,21} In most cases, a linearly polarized He–Ne laser has been used as an excitation source because of the larger absolute value of the real part of the dielectric constant in the metal layer at relatively long wavelengths (632.8 nm).²² In our previous paper,²⁰ the anodic photocurrent generated by photoinduced electron transfer between the LB film of the $\text{Ru}(\text{bpy})_3^{2+}$ copolymer and TEOA in an electrolyte solution was amplified dramatically under surface plasmon excitation using a blue laser beam at 441.6 nm.

In this study, we investigate the mechanism of enhancement of the anodic photocurrent generated by photoinduced electron transfer between the LB film of the $\text{Ru}(\text{bpy})_3^{2+}$ copolymer deposited on a silver electrode and TEOA in an electrolyte solution. The incident photon-to-current conversion efficiency (IPCE) is determined, and the advantage of surface plasmon excitation is discussed.

Experimental Section

Materials. *N*-dodecylacrylamide (DDA) was synthesized in chloroform by the reaction of acryloyl chloride and dodecylamine in the presence of triethylamine.²³ The product was purified by column chromatography extraction and subsequent recrystallization. Poly(*N*-dodecylacrylamide) (pDDA) was pre-

* To whom correspondence should be addressed. E-mail: miya@tagen.tohoku.ac.jp. Phone: +81-22-217-5637. Fax: +81-22-217-5642.

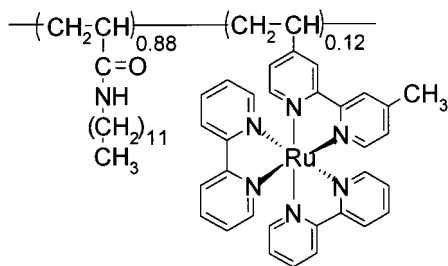


Figure 1. Chemical structure of amphiphilic copolymer containing $\text{Ru}(\text{bpy})_3^{2+}$ derivative (p(DDA-Ru)).

pared in distilled benzene at 60 °C by free-radical polymerization of DDA with 2,2'-azobisisobutyronitrile (AIBN) as a thermal initiator. The polymer was purified by precipitation into a large excess of acetonitrile and dried under vacuum at room temperature.

$\text{Ru}(\text{bpy})_3^{2+}$ copolymer was prepared as follows. 4-Vinyl-4'-methyl-2,2'-bipyridine (Vbpy) was synthesized according to published procedures.^{17,24} A copolymer of DDA with Vbpy was prepared by regular free-radical polymerization in distilled toluene at 60 °C with AIBN. The copolymer was purified by reprecipitation from the chloroform solution into a large excess of acetonitrile and dried for 12 h under vacuum at room temperature. The resulting copolymer was then refluxed with $\text{Ru}(\text{bpy})_2\text{Cl}_2$ in *n*-butanol for 72 h. The complex formation reaction was monitored via a decrease in the absorbance at 540 nm assigned to $\text{Ru}(\text{bpy})_2\text{Cl}_2$ and an increase in the absorbance at 450 nm corresponding to the MLCT band for $\text{Ru}(\text{bpy})_3^{2+}$. The counter chloride ions were replaced with more hydrophobic perchlorate ions by pouring the reaction mixture into a large excess of NH_4ClO_4 methanol solution. The copolymer-containing ruthenium complex (p(DDA-Ru)) was purified twice by reprecipitation in a large excess of ethyl acetate from the chloroform solution. The mole fraction of Ru complex in p(DDA-Ru) (Figure 1) was determined to be 0.12 from the UV–vis absorption spectrum. The molar absorption coefficient of $\text{Ru}(\text{bpy})_3^{2+}$ was used as a standard for determination of the copolymer composition: $\epsilon = 1.4 \times 10^4 \text{ M}^{-1} \text{ cm}^{-1}$ at 453 nm.

Monolayer and LB Film Formation. Measurement of surface pressure (π) – area (A) isotherms and the deposition of the monolayers were carried out using an automated Langmuir trough with a Wilhelmy-type film balance (HBM-AP, Kyowa Interface Science Co. Ltd.) at 15 °C. Distilled and deionized water (Milli-Q, Millipore) was used for the subphase. Quartz substrates, indium tin oxide (ITO) electrodes, and silver electrodes on glass were employed as substrates for monolayer deposition. The ITO electrode was washed in a chemical detergent solution, followed by chloroform and then acetone. The quartz substrate was treated with a UV– O_3 cleaner (NL-UV253, Nippon Laser and Electronics Laboratory). For surface plasmon measurement, high refractive index glass plates (LaSFn8, $n = 1.859$ at 436 nm) were immersed in a chloroform solution containing a few volume-percent octyltrichlorosilane in order to form hydrophobic surfaces. A chromium layer of 1.0 nm thickness was deposited using an electron gun (EGP-230, Anelva) onto the substrates in a vacuum of 1.9×10^{-4} Pa. A silver layer (ca. 40 nm) was then thermally deposited in the same chamber (V-KS200, Osaka Vacuum Ltd.). The thickness of each metal layer was monitored during deposition using a quartz crystal microbalance (XTM/2, Leybold Inficon). Finally, a p(DDA-Ru) monolayer was transferred onto the substrate by the vertical dipping method at a dipping speed of 5 mm min^{-1} at a surface pressure of 30 mN m^{-1} and temperature of 15 °C.

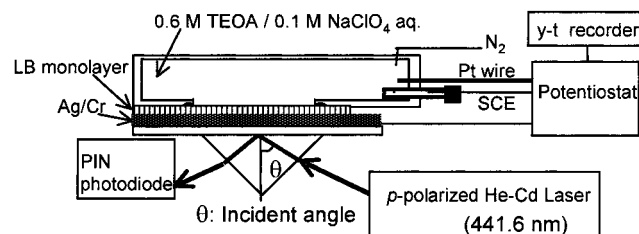


Figure 2. Schematic configuration of photocurrent measurement system combined with surface plasmon spectrometer.

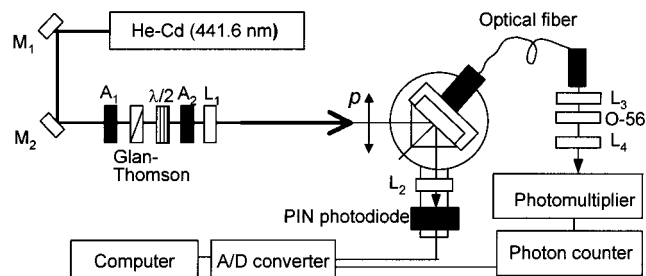


Figure 3. Schematic of photon counting system. M: half mirror. A: aperture. L: focusing lens.

Spectroscopy and Photocurrent Measurements. UV–vis absorption spectra were measured using a Hitachi U-3000 UV–vis absorption spectrometer. Emission spectra were measured using a Hitachi F-4500 spectrofluorophotometer. A schematic of the setup for reflectivity and photocurrent measurements is shown in Figure 2; the glass substrate on the opposite side of the silver electrode modified with the p(DDA-Ru) monolayer was coupled with a prism (LaSFn17, $n = 1.909$ at 441.6 nm) via matching oil in a Kretschmann configuration.²⁵ The silver electrode coupled with the prism was connected to a photoelectrochemical cell containing an electrolyte solution and mounted on a goniometer controlled via a personal computer.^{22,26} A linearly *p*-polarized He–Cd laser beam at 441.6 nm (IK5451R–E, Kimmon Electric Co. Ltd.) was used as an incident beam, with a diameter of 5 mm. Reflected light from the silver electrode was collected by a PIN photodiode and converted into a value of reflectivity using an A/D conversion system. Photocurrent measurement was carried out using the photoelectrochemical cell–silver electrode system, for which the applied potential was controlled using a potentiostat (366A, EG&G). The silver electrode modified with the p(DDA-Ru) monolayer, a saturated calomel electrode (SCE), and a platinum wire were used as a working electrode, a reference electrode, and a counter electrode, respectively. An aqueous solution of 1.0 M NaClO_4 and 0.6 M TEOA was used as the electrolyte solution. The electrolyte solution was bubbled with nitrogen gas for 10 min prior to the measurement of photocurrent. Emission intensity measurements were carried out using a single-photon counting system (C1230, HAMAMATSU; Figure 3). The emitted light from the Ru moiety was collected by a photomultiplier (R649S, HAMAMATSU) via a quartz optical fiber. A color filter (O-56, HOYA) was set in front of the photomultiplier to eliminate scattered light. All measurements were carried out at room temperature.

Results and Discussion

Formation of Langmuir–Blodgett Film Monolayer. The behavior of the p(DDA-Ru) monolayer was investigated by measuring the surface pressure–area isotherm. The isotherm reveals a steep rise in surface pressure and high collapse pressure, representing the formation of a densely packed stable

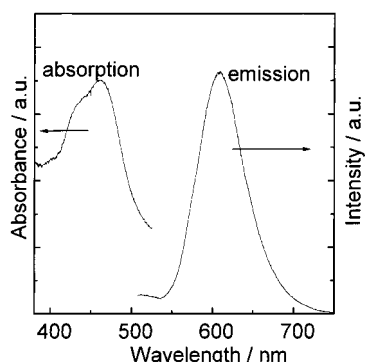


Figure 4. Absorption and emission spectra of the p(DDA-Ru) LB film with 30 layers on a quartz substrate. Excitation wavelength: 442 nm.

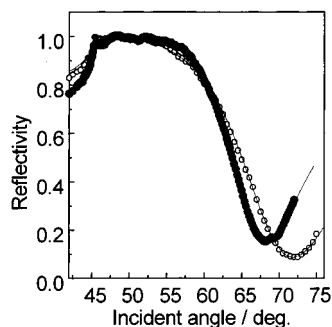


Figure 5. Reflectivity curves of bare silver electrode (closed circles) and p(DDA-Ru) monolayer on silver electrode (open circles) in a 1.0 M NaClO₄ aqueous solution containing 0.6 M TEOA. Solid lines: Fresnel fits.

monolayer at the water surface, as reported in the previous study.¹⁷ The average molecular occupied surface area of p(DDA-Ru) was 0.28 nm² per repeating unit, obtained by extrapolation of the linear part of the π -A isotherms to zero surface pressure. The cross-sectional area of the Ru(bpy)₃²⁺ derivative has been reported to be ca. 1.0 nm² molecule⁻¹.²⁷ The smaller surface area of p(DDA-Ru) indicates that the hydrophilic Ru(bpy)₃²⁺ group is placed in the water subphase. The p(DDA-Ru) monolayers were transferred onto a quartz substrate, an ITO electrode, and a silver electrode on both downward and upward strokes with a transfer ratio of unity, forming Y-type LB films. The absorption and emission spectra of the p(DDA-Ru) LB film with 30 layers deposited onto a quartz substrate are shown in Figure 4. The absorbance at 460 nm is assigned to the MLCT band of Ru(bpy)₃²⁺. The highest observed emission band was 610 nm, assigned to the typical emission band of Ru(bpy)₃²⁺. These findings show that Ru(bpy)₃²⁺ group is uniformly distributed in polymer LB films.

To monitor SPR generation at a silver surface, angular scans of reflectivity for a bare silver electrode and for the silver electrode coated with the p(DDA-Ru) monolayer were carried out in contact with an electrolyte solution. The reflectivity curves exhibit the same critical angle (θ_c) for total internal reflection of 45.60°, and dips (θ_R) at 68.00° (silver) and 72.00° (p(DDA-Ru) on silver; Figure 5). The dip is caused by energy transfer from evanescent light to surface plasmons at the silver surface by SPR generation, resulting in the decrease in reflected light energy. The dip of the monolayer deposited on the silver electrode was shifted toward higher angles compared with that of the bare silver electrode, attributable to the higher dielectric constant of the monolayer. The dielectric constant and thickness of each layer were determined by fitting the theoretical calculation based on Fresnel's equation to the experimental data (Table 1). The dielectric constants of chromium and silver were

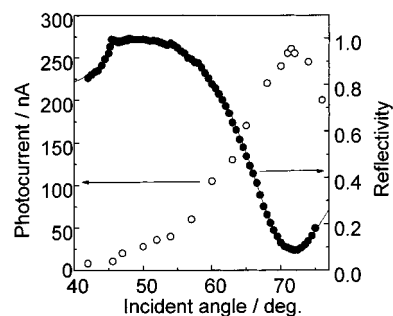


Figure 6. Steady-state anodic photocurrent (open circles) and reflectivity (closed circles) of the p(DDA-Ru) monolayer on silver electrode in a 1.0 M NaClO₄ aqueous solution containing 0.6 M TEOA. The photocurrent was measured at 0.0 V (vs SCE). The irradiation source was a *p*-polarized He-Cd laser beam (441.6 nm). The laser power was controlled at 7.56 mW using ND filters.

TABLE 1: Dielectric Constant and Film Thickness for Each Layer Determined from Fresnel Fits

layer	ϵ'	ϵ''	thickness (nm)
Cr	-12.1	12.0	1.5
Ag	-5.75	0.45	34.5
p(DDA-Ru)	+2.80	0.30	1.98
electrolyte solution	+1.83	0.0	

calculated to be $-12.1 + 12.0i$ and $-5.75 + 0.45i$, respectively. These values are consistent with published values.^{28,29} The thickness of the pDDA monolayer has been reported to be 1.8 nm based on X-ray diffraction measurements.²³ Therefore, the thickness of the p(DDA-Ru) monolayer determined here (1.98 nm) is reasonable, and the deposition of a p(DDA-Ru) monolayer on the silver electrode was confirmed.

Photocurrent Generation by SPR. The photocurrent generated by the silver electrode coated with the p(DDA-Ru) monolayer was measured by irradiating the electrode through a high refractive index prism in the presence of a TEOA electron donor agent in an electrolyte solution. The steady-state photocurrent for the p(DDA-Ru) monolayer on the electrode as a function of incident light angle (7.56 mW, 441.6 nm) at 0.0 V (vs SCE), in a nitrogen atmosphere is shown in Figure 6. The incident light is totally reflected at θ_c (45.6°), therefore, no direct excitation of Ru(bpy)₃²⁺ by incident light occurs. However, an anodic photocurrent (11 nA) is observed at θ_c . The anodic photocurrent generation is explained as follows. The evanescent wave, produced at the glass-metal interface at θ_c , excites Ru(bpy)₃²⁺ in the monolayer, and the resulting electron transfer from the TEOA electron donor in the electrolyte solution generates photocurrent (Figure 7a). Above θ_c , the photocurrent increases rapidly up to a maximum of 260 nA at 71.50°, which is slightly lower than the angle for minimum reflectivity (72.00°) (Figure 7b). This photocurrent is larger than that measured at θ_c by 23.6 times. It is interesting that the anodic photocurrent due to photoinduced electron transfer between excited Ru(bpy)₃²⁺ and TEOA is effectively enhanced by SPR. The photocurrent then decreases as the incident angle becomes higher. That is, the surface electromagnetic field at the metal-dielectric interface increases dramatically as the resonance condition associated with the excitation of the surface plasmon is approached and then decays again.⁸ The angle for the maximum photocurrent is slightly different from that for the minimum reflectivity. The difference is attributed to the fact that the anodic photocurrent is enhanced at the interface, whereas the reflectivity results from the interference of the reflected light generated from each layer.

The steady-state photocurrent at a fixed angle (71.50°) linearly increases with light intensity (Figure 8). The photocurrent

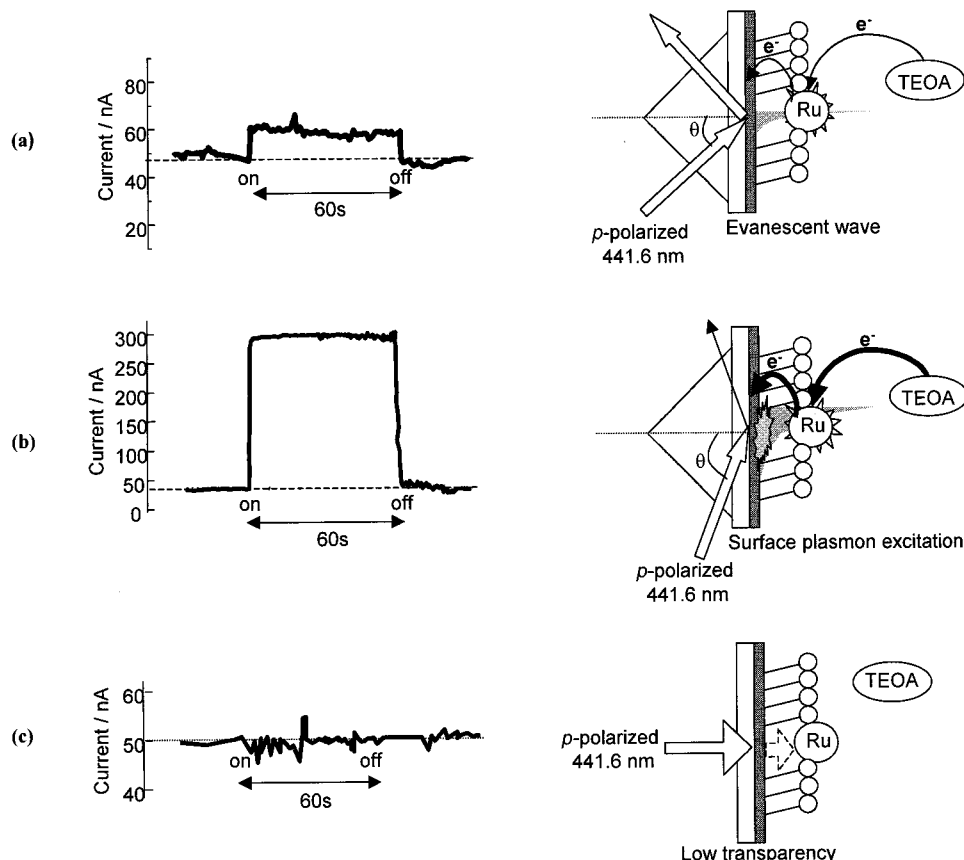


Figure 7. Photocurrent responses for the p(DDA-Ru) monolayer on a silver electrode at θ_c of 45.60° (a), 71.50° (b), and 0.00° without a prism (c) in a 1.0 M NaClO₄ aqueous solution containing 0.6 M TEOA. The applied potential was 0.0 V (vs. SCE), and the irradiation source was a *p*-polarized He–Cd laser beam (441.6 nm, 7.56 mW).

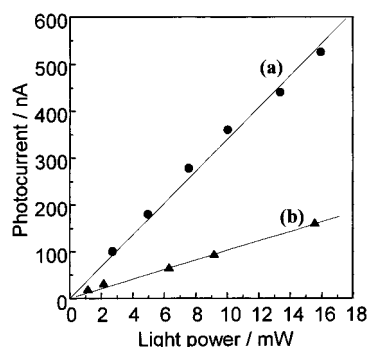


Figure 8. Dependence of anodic photocurrent on light power for the p(DDA-Ru) monolayer on silver (a) and ITO (b) electrodes in a 1.0 M NaClO₄ aqueous solution containing 0.6 M TEOA. The applied potential was 0.0 V (vs. SCE).

generation at 71.50° by SPR is more efficient compared with the case of the p(DDA-Ru) monolayer on a transparent ITO electrode when measured in the same electrolyte solution at 0.0 V (vs SCE) under irradiation using direct-transmitted light at 441.6 nm. The incident monochromatic photon-to-current conversion efficiency (IPCE) is defined as the number of electrons generated by irradiation in the external circuit divided by the number of incident photons. The IPCE value at 71.50° by SPR is calculated to be $9.53 \times 10^{-3} \%$ from the relation

$$\text{IPCE} = \frac{i/e}{n} \times 100 \quad (1)$$

$$n = \frac{W}{hc/\lambda} \quad (2)$$

where i is the photocurrent, e is the elementary charge, n is the number of incident photons, W is light power, h is the Planck constant, c is the velocity of light, and λ is the wavelength of the irradiation light. For comparison, we measured the photocurrent for the corresponding cell under conventional transmitted mode without a prism (Figure 7c). The photocurrent, however, was hardly detected under this condition. This is due to the low transmittance of the silver electrode as a result of absorption of the light and light-scattering by the silver layer. The IPCE value of the p(DDA-Ru) monolayer on the transparent ITO electrode is $2.87 \times 10^{-3} \%$ under conventional transmitted mode. The IPCE value for the SPR system is at least 3 times higher than that for conventional transmitted mode. Therefore, the excitation of Ru(bpy)₃²⁺ by SPR effectively improves the anodic photocurrent compared with the conventional direct irradiation system.

Emission Intensity Measurement. To understand the enhancement of the photocurrent by SPR in detail, the angular dependence of the emission intensity from p(DDA-Ru) LB films with four layers was measured in air (Figure 9a). The maximum emission intensity was obtained at an incident angle of 29.00°, which is slightly smaller than that for the minimum for reflectivity (29.60°). Figure 9a indicates that the concentration of photoexcited Ru(bpy)₃²⁺ increases as the reflectivity decreases, that is, the magnitude of SPR increases. Therefore, the enhancement of photocurrent generation observed in Figure 6 can be concluded to be caused by an increase in the concentration of excited Ru(bpy)₃²⁺ by SPR. The enhancement of the electromagnetic field at the silver surface by SPR was also demonstrated by theoretical calculations. The enhancement factor for the field intensity is given by the ratio of the field intensity at the silver surface under SPR to the incoming field

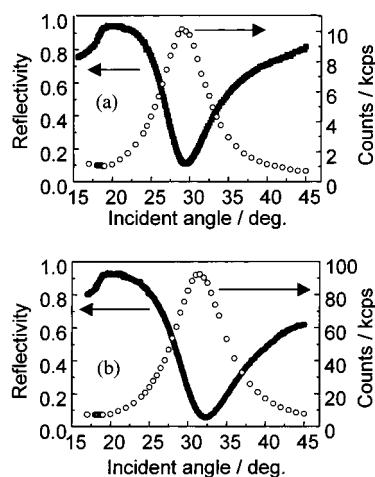


Figure 9. Emission intensity and reflectivity of the p(DDA-Ru) film with four layers (a) and the pDDA film with two layers and the p(DDA-Ru) film with four layers (b) on a silver electrode as a function of incident angle.

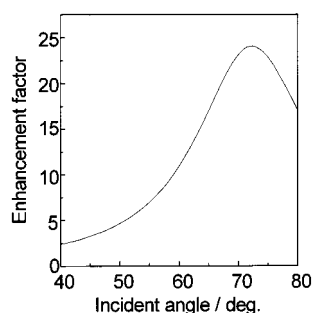


Figure 10. Enhancement factor of electric field intensity for the silver surface in a 1.0 M NaClO₄ aqueous solution containing 0.6 M TEOA as a function of incident angle. Silver thickness: 34.5 nm.

intensity in the glass substrate for *p*-polarized light. The enhancement factor as a function of incident angle was calculated using the thickness and dielectric constant for the silver electrode, the prism, and the electrolyte solution listed in Table 1.²¹ The maximum enhancement of electric field intensity at the silver layer thickness of 34.5 nm is estimated to be approximately 24 times (Figure 10). This is consistent with the results for the enhancement of photocurrent and emission intensity by SPR.

It is well-known that excited species produced on a metal surface by SPR are often quenched by the metal surface. To avoid such quenching of photoexcited Ru(bpy)₃²⁺ by the silver surface, we deposited the pDDA homopolymer LB film prior to the deposition of the p(DDA-Ru) LB film. An apparent enhancement of emission intensity was observed in specimens with this precoating (Figure 9b). Emission increases by a factor of approximately 9 compared with that of the sample without the pDDA layers. The thickness of the pDDA LB films with two layers is estimated to be 3.6 nm by X-ray diffraction measurements.²³ Therefore, the quenching of photoexcited Ru(bpy)₃²⁺ is avoidable by maintaining a distance of only a few nanometers from the silver. This distance may be adjusted by controlling the number of deposited pDDA layers. Such arrangement is a superior feature of the Langmuir–Blodgett technique. We are currently performing a detailed optimization of the silver electrode–Ru(bpy)₃²⁺ distance using the Langmuir–Blodgett technique.

Conclusion

Photocurrent generation based on photoexcited Ru(bpy)₃²⁺ by SPR was efficiently enhanced compared with conventional direct light irradiation. The photocurrent generated by SPR excitation at 71.50° was enhanced by 23.6 times that generated in total internal reflection mode. Moreover, it was observed that the quenching of photoexcited Ru(bpy)₃²⁺ on the silver surface is suppressed by precoating with pDDA LB layers, thereby maintaining an appropriate distance between the Ru(bpy)₃²⁺ and the silver surface. From these results, further enhancement of photocurrent generation is expected by placement of the Ru(bpy)₃²⁺ layer at a suitable distance from the silver surface, achieving effective SPR excitation using a metal electrode while ensuring less quenching by the metal electrode. The Langmuir–Blodgett technique is one of the most useful methods for engineering controlled film structures based on pDDA homopolymer and p(DDA-Ru) copolymer.

Acknowledgment. This work was supported in part by a Grant-in Aid for Scientific Research (No. 12450342) from the Ministry of Education, Culture, Sports, Science, and Technology of Japan.

References and Notes

- (1) Knoll, W. *MRS Bull.* **1991**, 16, 29.
- (2) Byrd, H.; Holloway, C. E.; Pogue, J.; Kircus, S.; Advincula, R. C.; Knoll, W. *Langmuir* **2000**, 16, 10322.
- (3) Ostuni, E.; Yan, L.; Whitesides, G. M.; *Colloids Surf. B* **1999**, 31, 3.
- (4) Chapman, R. G.; Ostuni, E.; Takayama, S.; Holmlin, R. E.; Yan, L.; Whitesides, G. M. *J. Am. Chem. Soc.* **2000**, 122, 8303.
- (5) He, L.; Musick, M. D.; Nicewarner, S. R.; Salinas, F. G.; Benkovic, S. J.; Natan, M. J.; Keating, C. D. *J. Am. Chem. Soc.* **2000**, 122, 9071.
- (6) Tsoi, P. Y.; Yang, J.; Sun, Y. T.; Sui, S. F.; Yang, M. *Langmuir* **2000**, 16, 6590.
- (7) Mitsuishi, M.; Li, T.; Miyashita, T. *Mol. Cryst. Liquid Cryst.* in press.
- (8) Liebermann, T.; Knoll, W. *Colloids. Surf. A* **2000**, 171, 115.
- (9) Ishida, A.; Sakata, Y.; Majima, T. *Chem. Commun.* **1998**, 57.
- (10) Bedja, I.; Hotchandani, S.; Kamat, P. V. *J. Phys. Chem.* **1994**, 98, 4133.
- (11) Yamada, K.; Kobayashi, N.; Ikeda, K.; Hirohashi, R.; Kaneko, M. *Jpn. J. Appl. Phys.* **1994**, 33, L544.
- (12) Yamada, S.; Kohrog, H.; Matsuo, T. *Chem. Lett.* **1995**, 639.
- (13) Kamat, P. V.; Bedja, I.; Hotchandani, S.; Patterson, L. K. *J. Phys. Chem.* **1996**, 100, 4900.
- (14) Argazzi, R.; Bignozzi, C. A.; Heimer, T. A.; Castellano, F. N.; Meyer, G. J. *J. Phys. Chem. B* **1997**, 101, 2591.
- (15) Nasr, C.; Kamat, P. V.; Hotchandani, S. *J. Phys. Chem. B* **1998**, 102, 10047.
- (16) Taniguchi, T.; Miyashita, T. *Chem. Lett.* **1997**, 295.
- (17) Miyashita, T.; Taniguchi, T.; Fukasawa, Y. *Chin. J. Polym. Sci.* **1999**, 17, 75.
- (18) Taniguchi, T.; Fukasawa, Y.; Miyashita, T. *J. Phys. Chem B* **1999**, 103, 1920.
- (19) Aoki, A.; Abe, Y.; Miyashita, T. *Langmuir* **1999**, 15, 1463.
- (20) Fukuda, N.; Mitsuishi, M.; Aoki, A.; Miyashita, T. *Chem. Lett.* **2001**, 378.
- (21) Raether, H. *Surface Plasmons on Smooth and Rough Surfaces and on Gratings*; Springer-Verlag: Berlin, 1988; Chapter 2.
- (22) Ishida, A.; Sakata, Y.; Majima, T. *Chem. Lett.* **1998**, 267.
- (23) Miyashita, T.; Mizuta, Y.; Matsuda, M. *Br. Polym. J.* **1990**, 22, 327.
- (24) Ghosh, P. K.; Spiro, T. G. *J. Am. Chem. Soc.* **1980**, 102, 5543.
- (25) Kretschmann, E. *Opt. Commun.* **1972**, 6, 185.
- (26) Badia, A.; Arnold, S.; Scheumann, V.; Zizlsperger, M.; Mack, J.; Jung, G.; Knoll, W. *Sens. Actuators, B* **1999**, 54, 145.
- (27) Zhang, X.; Bard, A. J. *J. Am. Chem. Soc.* **1989**, 111, 8098.
- (28) Prucha, E. J.; Kaminow, I. P. *Handbook of Optical Constants of Solids II*; Academic Press: San Diego, 1998.
- (29) Schroder, U. *Surf. Sci.* **1981**, 102, 118.